DOI: 10.1002/JLB.1A0920-588R

ARTICLE

JLB JOURNAL OF LEUKOCYTE BIOLOGY

Loss of mTORC2-induced metabolic reprogramming in monocytes uncouples migration and maturation from production of proinflammatory mediators

Maryam Jangani[1] | Juho Vuononvirta[1] | Lamya Yamani[2] | Eleanor Ward[1] | Melania Capasso[2,3] | Suchita Nadkarni[1] | Frances Balkwill[2] | Federica Marelli-Berg[1]

[1] William Harvey Research Institute, Barts and The London School of Medicine and Dentistry, Queen Mary University of London, Charterhouse Square, London, UK

[2] Barts Cancer Institute, Barts and The London School of Medicine and Dentistry, Queen Mary University of London, Charterhouse Square, London, UK

[3] German Center for Neurodegenerative Diseases (DZNE) within the Helmholtz Association, Bonn, Germany

Correspondence
Federica Marelli-Berg, William Harvey Research Institute, Barts and The London School of Medicine and Dentistry, Queen Mary University of London, Charterhouse Square, London EC1M 6BQ, UK.
Email: f.marelli-berg@qmul.ac.uk

Abstract

Monocyte migration to the sites of inflammation and maturation into macrophages are key steps for their immune effector function. Here, we show that mechanistic target of rapamycin complex 2 (mTORC2)-dependent Akt activation is instrumental for metabolic reprogramming at the early stages of macrophage-mediated immunity. Despite an increased production of proinflammatory mediators, monocytes lacking expression of the mTORC2 component Rictor fail to efficiently migrate to inflammatory sites and fully mature into macrophages, resulting in reduced inflammatory responses in vivo. The mTORC2-dependent phosphorylation of Akt is instrumental for the enhancement of glycolysis and mitochondrial respiration, required to sustain monocyte maturation and motility. These observations are discussed in the context of therapeutic strategies aimed at selective inhibition of mTORC2 activity.

KEYWORDS
cell metabolism, mTORC2, monocyte, macrophage, metabolism

1 | INTRODUCTION

Extravasationand tissue infiltration[1–3] and their further maturation into tissue macrophages[4,5] are crucial to monocyte function. Once in the tissue, a variety of soluble mediators and signaling pathways determine monocyte differentiation into proinflammatory or prohealing macrophages, which contribute to progression and resolution of the inflammatory process, respectively.

In myeloid cells, the PI3K–mechanistic target of rapamycin (mTOR) signaling pathway is activated by TLR ligands and cytokines and controls functional differentiation of monocytes and macrophages.[6–9] Importantly, macrophage differentiation is intrinsically linked to metabolic remodeling,[10] which is also regulated by the PI3K–mTOR pathway.[11]

mTOR serves as a core component of 2 distinct protein complexes, mTOR complex 1 (mTORC1) and mTOR complex 2 (mTORC2), which regulate different cellular processes.

Regulatory-associated protein of mTOR (Raptor) functions as an adapter protein and kinase in the mTORC1 complex, whereas rapamycin-insensitive companion of mTOR (Rictor) is an obligatory component of mTORC2, required for Akt/protein kinase B phosphorylation on Serine473.

The role of mTORC1 in regulating differentiation, inflammation, and metabolism in monocytes and macrophages has been intensively studied.[12–14] Specifically, the mTORC1 pathway has been linked to the activation of glycolysis and the acquisition of a

Abbreviations: PI3K, Phosphoinositide 3-kinase; mTOR, mammalian target of Rapamycin; mTORC2 (Rictor), mTORC complex 2; HIF1alpha, Hypoxia Inducible Factor 1 alpha

proinflammatory phenotype. In monocytes, β-glucansstimulate the AKT–mTORC1–HIF1α axis, resulting in a shift from oxidative phosphorylation (oxphos) toward glycolysis.[15] mTORC1-depedent hexokinase (HK1)-mediated glycolysis is indispensable for NLRP3 inflammasome activation and subsequent IL-1β and IL-18 expression in macrophages.[16]

Like mTORC1, mTORC2 has been linked to the regulation of glycolysis and oxphos in myeloid cells. mTORC2 activity in myeloid cells, however, appears to promote an anti-inflammatory phenotype. In macrophages, deletion of Rictor led to reduced glycolysis and oxphos and inhibition of M2 activation upon IL-4 stimulation.[17] More recently, TCA cycle-related genes were shown to be up-regulated in IL-4-treated monocyte-derived macrophages from mTORC2-deficient mice.[18] Upon activation, Rictor-deficient macrophages have been reported to undergo a dramatic shift toward a proinflammatory phenotype, and secrete high levels of cytokines such as TNF-α and IL-6.[19]

Despite these observations, the effect of mTORC2 on the inflammatory response in vivo remains unclear.[19]

In this study, we investigated the contribution of mTORC2 to distinct early events of monocyte/macrophage-mediated inflammation, namely cell migration and functional maturation. Our data are consistent with an essential role of mTORC2, but not mTORC1, in sustaining migration of monocytes to inflammatory sites and their subsequent maturation via metabolic reprogramming. Importantly, loss of mTORC2-regulated functions outweighs the proinflammatory differentiation of Rictor-deficient macrophages in vivo, resulting in an impaired inflammatory response.

2 | METHODS

2.1 | Mice

Rictor$^{Lox/Lox}$ and Raptor$^{Lox/Lox}$ mice were gifts from (Prof. Dr. Markus Rüegg). The CSF1R-cre ER$^{+/-}$ transgenic mice [B6.129P2-Lyz2tm1(cre)Ifo/J; Jackson Laboratory] were back crossed with C57BL6 mice 5 times and then crossed with either Rictor$^{Lox/Lox}$ or Raptor$^{Lox/Lox}$ mice to obtain heterozygous CSF1R-cre$^{+/-}$; Rictor$^{Lox/Wt}$ or Raptor$^{Lox/Wt}$ offspring (where WT refers to wild type) as F1 generation. These heterozygous mice were crossed to obtain the -Rictor-CSF1Rcre*ER*$^{+/-}$ (referred to here as CSF1R-cre Rictor^{KO}) with genotype CSF1R-creER$^{+/-}$; Rictor$^{Lox/Lox}$ or CSF1R-creER$^{+/-}$; Raptor$^{Lox/Lox}$. The littermates that are CSF1R-cre ER$^{+/-}$ (referred to here as CSF1R-creER Rictor^{WT}) were used as control WT mice. For all mice used, the genotypes were determined by PCR analysis of earpiece by a commercial vendor (Transnetyx). To obtain the CSF1R-cre Rictor^{KO} macrophages, following intraperitoneal tamoxifen administration for 3 days, bone marrows (BM) were extracted, and macrophages were matured for 7 days (Figure S1(A)) with 20 ng/ml M-CSF. All in vivo experiments were conducted with strict adherence to the Home Office guidelines following approval by the Queen Mary University of London Ethics committee.

2.2 | Reagents

All reagents and resources used in this study are summarized in Table S1.

2.3 | BM-derived macrophage culture

Bone marrow derived macrophages (BMDMs) originated from hematopoietic progenitors in the BM and are differentiated into mature macrophages in the presence of Refs. [20] and [21]. For BMDM isolation, mice were sacrificed and both tibias and femur were collected. Skin and muscles were removed and the bones were washed in 70% ethanol. BM was flushed out the bones using a syringe filled with BMDM growth media DMEM, high glucose (Thermofisher; cat# 11965092), supplemented with 10% FBS and 1% penicillin/streptomycin. To differentiate the BM cells into mature macrophages, we used 20 ng/ml mouse MCSF (eBioscience; cat# 14-8983-80). The cells were incubated for 7 days in a humidified 5% CO_2 incubator at 37°C until fully differentiated. They were then washed with PBS + 2 mM EDTA. The adhered BMDMs were scraped off the plate and washed with DMEM before seeding for the target assays!

2.4 | Phagocytosis in BMDMs

BMDMs were grown to confluence and then plated at 1×10^6 cells/well in 6-well plates. BMDMs were treated with 100 ng/ml LPS and 20 ng/ml IFNγ overnight before addition of IgG-coated carboxylate-modified flouromicrospheres 1.0 μm (Thermofisher; cat# F-8823) for up to 90 min. Phagocytosis was stopped by incubating cells with ice cold PBS. Ingested particles were visualized by flow-cytometer analysis on the yellow-green channel. Mean fluorescence intensity of the ingested particles were expressed as fold over no LPS (media) after taking away the ice control sample. For F actin and G actin analysis, the LPS/IFNγ-treated BMDMs were incubated with microspheres for the indicated times and then fixed with 3.7% formaldehyde. BMDMs were permeabilized with 0.3% Triton-X and then stained with phalloidin actin (Alexa Fluor™ 488 Phalloidin; Thermofisher; cat# A12379) and G actin (Deoxyribonuclease I, Alexa Fluor™ 594 Conjugate Thermofisher; cat# D12372). The fluorescence was analyzed by flow cytometry. Alternatively, cells were imaged by confocal microscopy (Zeiss LSM710). For quantification, the mean fluorescence intensity of F-actin and G-actin are presented as a ratio.

2.5 | Peritonitis model

CSF1R-cre Rictor^{KO} and CSF1R-creER Rictor^{WT} mice were injected i.p. with 500 μl of sterile 3% thioglycollate medium brewer modified (TG) (BD Bioscience; cat# B11716) or 1 mg/ml zymosan (Sigma; cat#

Z4250). Mice were monitored throughout the experiment for signs of discomfort. Mice were sacrificed either 24 or 72 h postinjection and peritoneal lavage cells collected by a peritoneal cavity wash under aseptic conditions with 10 ml of sterile PBS and processed for flow cytometry!

2.6 | Tracking labeled monocyte in a model of peritoneal inflammation

CSF1R-cre Rictor^{KO} and CSF1R-creER Rictor^{WT} mice were sacrificed after 3 days tamoxifen treatment. The BM was washed with MACS buffer: PBS, 1% FBS and 2 mM EDTA. The RBCs were lysed and monocytes were isolated with Monocyte Isolation Kit (BM) (Miltenyi; cat# 130-100-629) according to the manufacturer's instruction. Monocytes were then counted and treated with either carbonyl cyanide 4-(trifluoromethoxy) phenylhydrazone (FCCP) 1 μM or 2-deoxy-D-glucose (2DG) 10 mM for 1 h and then labeled with either Cell Tracker™ Orange CMRA Dye (Thermofisher; cat# C34551) and injected i.v. into tail vein. The recipient mice were then injected i.p. with 1 mg/ml zymosan. Twenty-hours postinjection, mice were sacrificed, and peritoneal lavage was collected for flow cytometry analysis.

2.7 | Migration assays

BMDMs were resuspended at 1×10^6 cells per ml in DMEM with 10% FBS. To measure chemotaxis 0.1 ml of cells was added to 6.5 mm diameter 5 μM pore size PET Transwell cell culture inserts (Costar; cat# 3421). To induce chemotaxis, 0.1×10^6 mouse embryonic fibroblasts or TB32047 pancreatic cancer cells were seeded on the bottom of the 24-well plate O/N prior to the experiment. BMDMs were allowed to migrate for 24, 48, or 72 h. Migrated cells on the bottom of the membrane were fixed in crystal violet with 2% methanol for 10 min. To measure transmigration, the inserts were incubated in 10% acetic acid for 10 min and absorbance read at 595 nm. Experiments were done in triplicates.

For monocyte transmigration assays, 0.1×10^6 cells were resuspended in RPMI + 10% FBS and added to insert while 50 ng/ml CCL2 (BioLegend; cat# 578402) was added to the lower chamber as the chemoattractant. The monocytes were left to migrate through the membrane for 2 h. The media above the membrane was first removed. The upper side of the membrane was then cleaned off thoroughly with a cotton wool. This ensured removal of any cells that did not migrate from analysis. Chemotaxis was measured by cutting the membrane, and fixing cells in formalin and counting the DAPI stained nuclei on the transwell bottom by immunofluorescence. The condition with the highest absorbance reading was set to 100% and others were calculated as a % of the highest value. For experiments using the metabolic modifying drugs, monocytes were pretreated with either 50 μm triciribine, 10 mM 2DG, 1 μM FCCP, 50 μM etomoxir (Sigma–Aldrich; cat# E1905) or 2 μM oligomycin before being exposed to 50 ng/ml CCL2 gradient for 2 h.

2.8 | Zymosan-induced paw inflammation

CSF1R-cre Rictor^{KO} and CSF1R-creER Rictor^{WT} mice were given 1 intraplantar injection of 20 μl of 200 μg zymosan (Sigma; cat# Z4250) in the left paw while the right paw received the 20 μl of vehicle only! The paw volume and diameter was measured every day for up to 3 days postinjection with a plethysmometer. Mice were sacrificed at end point and both paws were collected, weighed, and digested with 1 mg/ml Collagenase D (Roche; cat# 11088858001) and 50 unit/ml DNase I (Sigma; cat# D4263). Digestion was stopped using 2 mM EDTA. Lysates were passed through 70 μm mesh strainers twice to remove any cellular debris. Cell count was performed prior to staining extracellular surface markers and processed for flow cytometry analysis.

2.9 | Western blotting

Whole cell lysates were lysed in 1× RIPA buffer (10 mM Tris–Cl (pH 8.0, 50 mM Tris pH 8.0, 1% Triton X-100, 0.5% sodium deoxycholate, 0.1% SDS, 150 mM NaCl + 1× phosphatase inhibitor cocktail 2 and 3 (Sigma–Aldrich; cat# P5726 and P0044) cat# 1× protease inhibitor cocktail set 1 (Merck Millipore; cat# 539131). Equivalent amounts of protein as determined by standard Bradford assay (Bio-Rad; cat# 5000001) were separated by SDS/PAGE and transferred to nitrocellulose membrane (GE Healthcare Life Sciences; cat# 10600002). Membranes were blocked for 2 h at room temperature in 5% milk/TBS-Tween 20 (Sigma; cat# P1379) and were incubated overnight at 4°C with the primary antibodies stated. HRP-conjugated secondary antibody (1:2500; Amersham Bioscience; cat# NA934) was subsequently added. Films were then developed. The intensity of the bands was quantified using ImageJ (NIH).

2.10 | qRT-PCR

Cells were lysed using RLT buffer and then total RNA extracted with Qiagen RNeasy mini Prep (Qiagen; cat# 74106) according to the manufacturer's instructions. RNA Quantity and quality was measured on NanoDrop spectrophotometer. Reverse transcription was performed according to the manufacturer's instruction (Applied Biosystems; cat# 4374966). Gene expression analysis was done using Taqman Gene expression Master Mix (Thermofisher; cat# 4369016) on the StepOne Plus Real Time PCR system (Thermofisher). Expression was calculated using the ΔΔCt method (Livak and Schmittgen, [2001])[22] and normalized to a housekeeping gene (B2M). Experiments were done in triplicates.

2.11 | Confocal microscopy

Cells were allowed to adhere onto poly-L-lysine coated coverslips and fixed in 4% paraformaldehyde (Thermo Fisher Scientific; cat# 28906) for 5–10 min at room temperature. Where mentioned,

permeabilization was carried out using 0.2% Triton X-100 (Sigma–Aldrich; cat# X100-500ML) in PBS for 5 min. Cells were then washed in PBS, blocked in blocking buffer (PBS containing 0.1% BSA; Sigma–Aldrich; cat# 05470) and 1% serum of the species giving rise to secondary antibodies) for 3–6 h and then stained with appropriate primary antibodies at 4°C for 16 h in the dark. Following staining, cells were washed again and stained with corresponding secondary antibodies and DAPI for 30 min at room temperature. After multiple PBS washes coverslips were mounted onto slides using ProLong Gold Antifade (Invitrogen/Life Technologies; cat# P36930) and then examined using a Leica SP5 confocal microscope equipped with a 63 × 1.4 NA objective. Confocal images and Z stacks were acquired and analyzed by confocal microscopy (Zeiss LSM710). Repositioning of scale bars and image layouts were prepared using Adobe Photoshop (Adobe Systems). All images in a group were treated equally.

2.12 | BMDM cytokine and activation molecules analysis

Cytokines were measured from cell culture media using commercial ELISA kits from BD Biosciences according to manufacturer's instructions. For cell surface marker analysis, 1×10^6 BMDMs were incubated with LPS/IFNγ for 6 h and then processed for flow cytometry analysis.

2.13 | Measurement of oxygen consumption rates and extracellular acidification rates

Real time bioenergetics analysis of extracellular acidification rates (ECAR) and oxygen consumption rates (OCR) of monocytes subjected to chemokine stimulation was performed using the XF analyzer (Seahorse Biosciences). Monocytes were cultured in serum free, unbuffered XF assay medium (Seahorse Biosciences; cat# 102365-100) for 1 h. The cells were then seeded (11×10^5/well) into the Cell Tak-treated seahorse XF96 cell plates for analysis. Monocytes received either CCL2 or media only vehicle at the start of the assay. Perturbation profiling of the use of metabolic pathways by monocytes was achieved by the addition of oligomycin (2 μM), FCCP (2 μM), rotenone and antimycin A (0.5 μM), 2DG (50 mM; all from Seahorse Biosciences; cat# 103020–100 and 103015–100). Experiments with the Seahorse system were done with the following assay conditions: 2 min mixture; 2 min wait; and 4–5 min measurement. Metabolic parameters were calculated. Experiments were done in at least 5 replicates and with at least 3 biologic repeats. For mitochondria activation and ROS production studies, 1×10^5 monocytes were pretreated with either 5 0μM Akt inhibitor (triciribine; Selleckchem; cat# S1117) for 1 h followed by 50 ng/ml CCL2 treatment. The cells were then washed and incubated with 150 nM MitoTracker Red CMXRos (Thermofisher; cat# M7512) or 2μM DCFDA (Thermofisher; cat# C369) for 30 min at 37°C. Excess dye was washed off and cells were analyzed by flow cytometry on PE and FITC channels, respectively.

2.14 | ATP assay

Monocytes from CSF1R-cre Rictor^{KO} and CSF1R-creER Rictor^{WT} mice were isolated and plated at 1×10^6 per well in triplicates. They were treated with either media only or 50 ng/ml CCL2 for 2 h. The cells were then lysed in 50 μl somatic cell ATP releasing reagent (Sigma; cat# FLSAR) and cellular ATP measured using the ATP determination kit (Thermofisher; cat# A22066) according to the manufacturer's instructions. The experiment was repeated with 3 biologic replicates.

3 | RESULTS

Loss of Rictor expression results in proinflammatory differentiation of macrophages in vitro, but reduced monocyte recruitment in vivo.

In this study, we aimed to investigate the effects of *Rictor* deletion on macrophage functions in vitro. It has been previously shown that mice lacking Rictor in both macrophages and neutrophils under the control of the LysMcre promoter become hypersensitive to TLR4 stimulation.[19] *Rictor-LysMcre KO* BMDMs produced significantly higher levels of inflammatory cytokines following exposure to LPS compared with their WT counterparts.[19] To prevent the deletion of all myeloid cells, we utilized the tamoxifen-inducible Cre recombinase under the control of CSF 1 receptor promoter (CSF1R-icre), specific for the monocyte and macrophage lineage[23] (Figures S1(A) and S1(B)). When crossed with *Rictor*$^{f/f}$ or *Raptor*$^{f/f}$ mice, *rictor* and *raptor* were deleted only in monocyte/macrophage lineage (Figure S1(C) and S1(D)). The lines were named CSF1R-icreER Rictor^{KO} and *CSF1R-icreER* Raptor^{KO}, respectively, whereas the littermates used as controls were CSF1R-icreER Rictor^{WT} or *CSF1R*-icreER Raptor^{WT}.

To assess the contribution of mTORC2 to monocyte/macrophage proinflammatory differentiation, BMDMs were exposed to LPS and IFNγ for 12 h in vitro. As shown in Figures 1(A)–1(E), CSF1R-icreER Rictor^{KO} BMDMs showed a marked increase in NOS2, IL-6, TNFα, and IL-12b production compared with CSF1R-icreER Rictor^{WT} BMDMs. Similarly, LPS and IFNγ stimulation of Raptor-deficient BMDMs resulted in a significant induction of transcription of proinflammatory cytokine genes *Tnfα*, *Il-12b*, and *Il-6* (Figures S1(E)–S1(I)). These findings are in line with similar previously reports[24,25] and further confirm a role for both complexes during the inflammatory response.

We subsequently sought to establish whether the proinflammatory effect of Rictor and Raptor deficiency could translate into an increase of the inflammatory response in vivo.

First, we examined paw volume and diameter over a period of up to 72 h in a zymosan-induced inflammation model. Zymosan is a TLR2 ligand that induces monocyte recruitment and cytokine release.[26] Both volume and diameter of the inflamed paw was mildly reduced in CSF1R-icreER Rictor^{KO} mice, albeit not significantly at all the time point examined (Figure 2(A) and Figure S2(A)). This was accompanied by a significant decrease in the number of macrophages in the inflamed paw of CSF1R-cre Rictor^{KO} mice compared with CSF1R-cre Rictor^{WT} mice (Figure 2(B)). The small decrease in paw swelling compared with

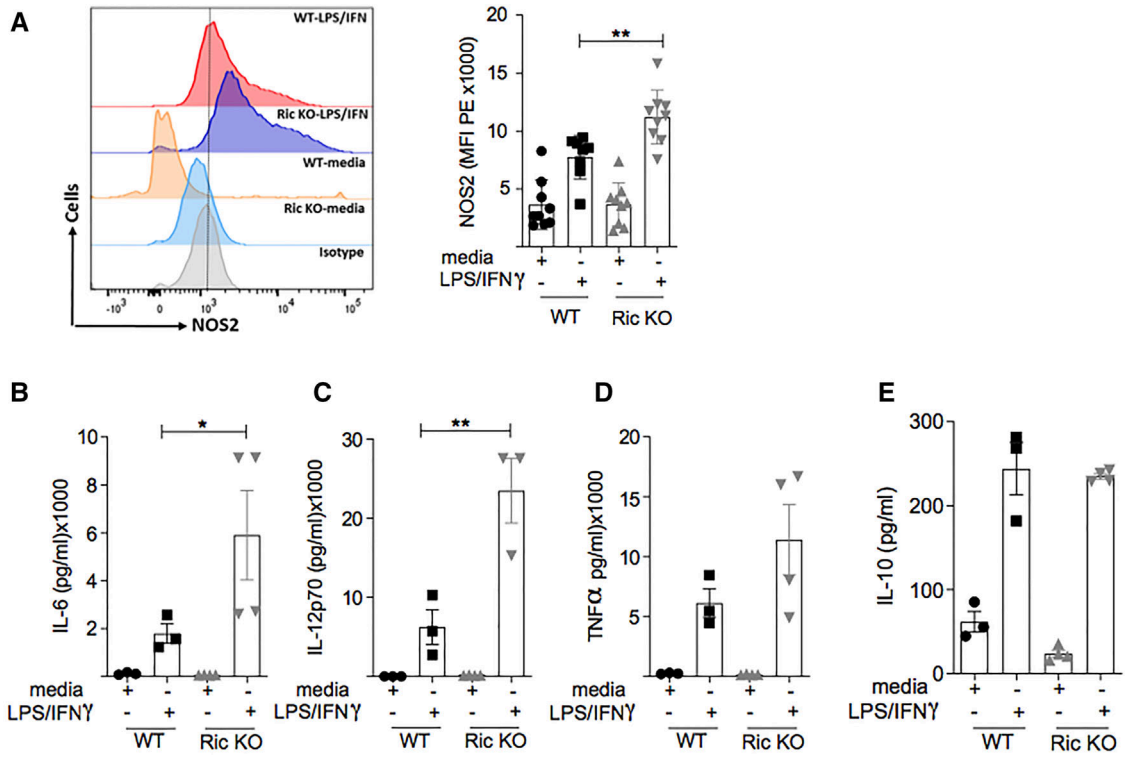

FIGURE 1 mTORC2 deficiency promotes a proinflammatory phenotype in macrophages. (A) BMDMs from *CSF1R-icreER Rictor*^{wt} (WT) or *CSF1R-icreER Rictor*^{ko} (Ric KO) mice were stimulated with LPS and IFNγ for 6 h. The expression of NOS2 was measured by flow cytometry and expressed as the mean fluorescent intensity (MFI) of PE channel ($n = 10$). (B)–(E) ELISA bar charts of cytokines measured in triplicates in BMDMs stimulated for 12 h with LPS/IFNγ. Minimum of $n = 3$ biologic replicates. Statistical test: unpaired *t*-test. $^{*}p < 0.05$ and $^{**}p < 0.001$

the more substantial reduction of infiltrating macrophages is probably due to intact microvascular permeability—as Rictor deficiency selectively affect monocytes in our model. Expression of CD11b, an important integrin involved in monocyte adhesion and migration, was comparable between the WT and Rictor-deficient groups (Figure 2(B)).

In addition, we observed a significant reduction in the FcγRI receptor (CD64) expression on the surface of infiltrating Rictor-deficient macrophages, indicating a defect in the maturation of *CSF1R-icreER Rictor*^{KO} monocytes that succeeded in infiltrating the tissue (Figure 2(C)).

No differences were observed in the vehicle-injected paw, irrespective of Rictor expression (Figure 2(A) and Figure S2(A)).

In line with the data described in Figure 1, zymosan-treated BMDMs displayed higher mRNA levels of the proinflammatory mediator IL-1β in the absence of mTORC2 activity Figure S2(C)).

To formally rule out potential effects of Rictor deficiency on resident macrophages, we further investigated migration of monocytes in thioglycollate-induced peritonitis, collecting migrating leukocytes as a single cell suspension from the peritoneal cavity. As shown in Figure 2(D), we employed a gating strategy to also monitor the maturation of migrated monocytes (CD11b^{+}, Ly6C^{+}) into macrophages (CD11b^{+}, Ly6C^{-} F4/80^{+}). The absolute number of monocytes in the peritoneal exudate of CSF1R-icreER Rictor^{KO} mice was significantly lower than that retrieved from CSF1R-icreER Rictor^{WT} littermates at 24 h (Figure 2(E)). Accordingly, the number of infiltrating macrophages was significantly reduced in the CSF1R-icreER Rictor^{KO} mice at 72 h (Figure 2(F)), reflecting the reduced number of migrating monocytes, which subsequently differentiated into macrophages. Reduced F4/80 expression intensity in the infiltrated macrophage population confirmed the defective maturation of CSF1R-icreER Rictor^{KO} monocytes (Figure 2(G)). In line with these observations, CD64 expression was lower in CSF1R-cre Rictor^{KO} mice (Figure 2(H)). As expected, the absolute number of neutrophils was unchanged (Figure S2(D)). The contribution of Rictor to monocyte maturation was confirmed by in vitro experiments in which stimulation of TLR4 (LPS and IFNγ) of BMDMs from CSF1R-cre Rictor^{WT} and CSF1R-cre Rictor^{KO} mice was ineffective in inducing up-regulation of CD86 and MHC II molecules (Figures S2(D) and S2(F)). We did not observe any differences on CD40 expression in CSF1R-cre Rictor^{KO} samples (Figure S2(F)).

Collectively these results indicate a role for mTORC2 in regulating both migration and differentiation of monocytes during an inflammatory immune response.

Rictor-deficient monocytes and macrophages show impaired cytoskeleton rearrangement in response to migratory stimuli.

As a first step to define the molecular mechanism of Rictor-mediated regulation of myeloid cell migration, the migratory ability of CSF1R-icreER Rictor^{KO} and CSF1R-icreER Rictor^{WT} BMDMs was investigated by in vitro migration assays. BMDMs from CSF1R-icreER

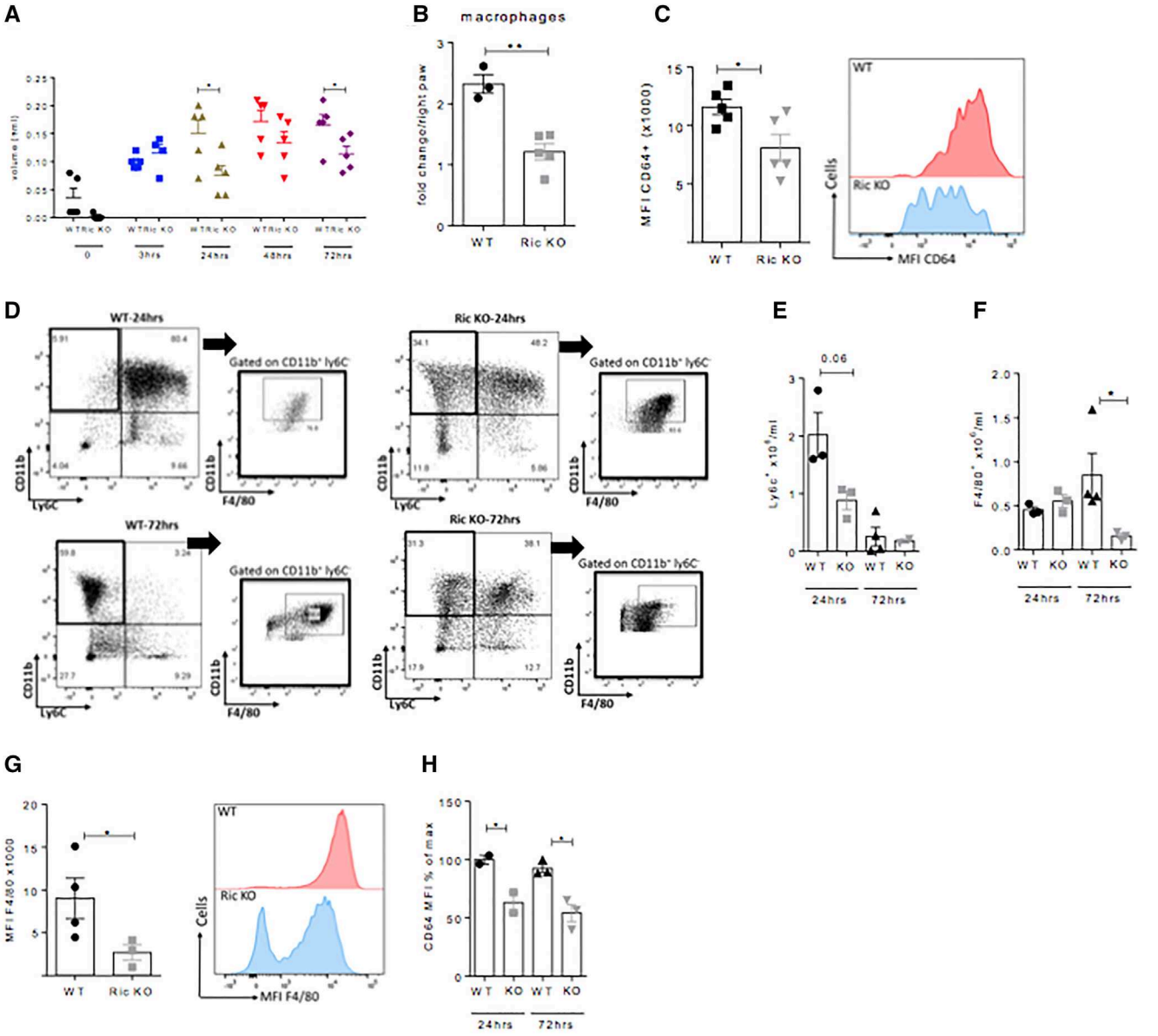

FIGURE 2 mTORC2 deficiency impairs monocyte recruitment in vivo. (A) WT or *CSF1R-icreER Rictor*^{ko} mice received intraplantar injection of either vehicle or zymosan. The volume of the inflamed of the paw was confirmed on a plethysmometer and measured by a caliper after 24, 48, and 72 h. (B) The number of infiltrating macrophages in the paw exudate was confirmed by flow cytometry at endpoint. (C) CD64 expression of infiltrated macrophages was analyzed by flow cytometry and expressed as MFI with histogram curve showing on the right. (D) WT or *CSF1R-icreER Rictor*^{ko} mice were given 1 intraperitoneal injection of 500 μl of Thioglycollate. The mice were sacrificed after 24 or 72 h and peritoneal lavage was taken for flow cytometry analysis. (E) and (F) Ly6C+ monocytes and F4/80+ macrophages were calculated and measured as absolute numbers per ml of lavage taken. (G) and (H) MFI of F4/80 and CD64 on peritoneal macrophages was analyzed. Experiments were done at least in triplicates. Statistical test: unpaired *t*-test, $^{*}p < 0.05$ and $^{**}p < 0.001$

Rictor^{KO} or CSF1R-icreER Rictor^{WT} mice were seeded onto transwell inserts over wells containing either fibroblasts or pancreatic cancer cell lines. As shown in Figures 3(A) and 3(B), CSF1R-icreER Rictor^{KO} BMDMs migrated significantly less across the membrane to either fibroblasts or cancer cells compared with CSF1R-icreER Rictor^{WT} cells (Figures 3(A) and 3(B)). We also analyzed the CSF1R-creER Raptor^{KO} BMDMs in in vitro migration assays and did not observe any difference between the Raptor-deficient and WT groups (Figure 3(C)).

These observations were further confirmed using the chemokine CCL2 to drive monocyte migration. As shown in Figure S3, loss of mTORC2 activity significantly reduced monocyte migration to this chemokine. In these experiments, zymosan alone did not induce monocyte migration, suggesting that the effects observed in the paw inflammation model are mediated by zymosan-induced chemokine production and subsequent monocyte chemotaxis.

Fast and efficient actin polymerization and cytoskeletal reorganization are essential steps regulating cellular motility in response to

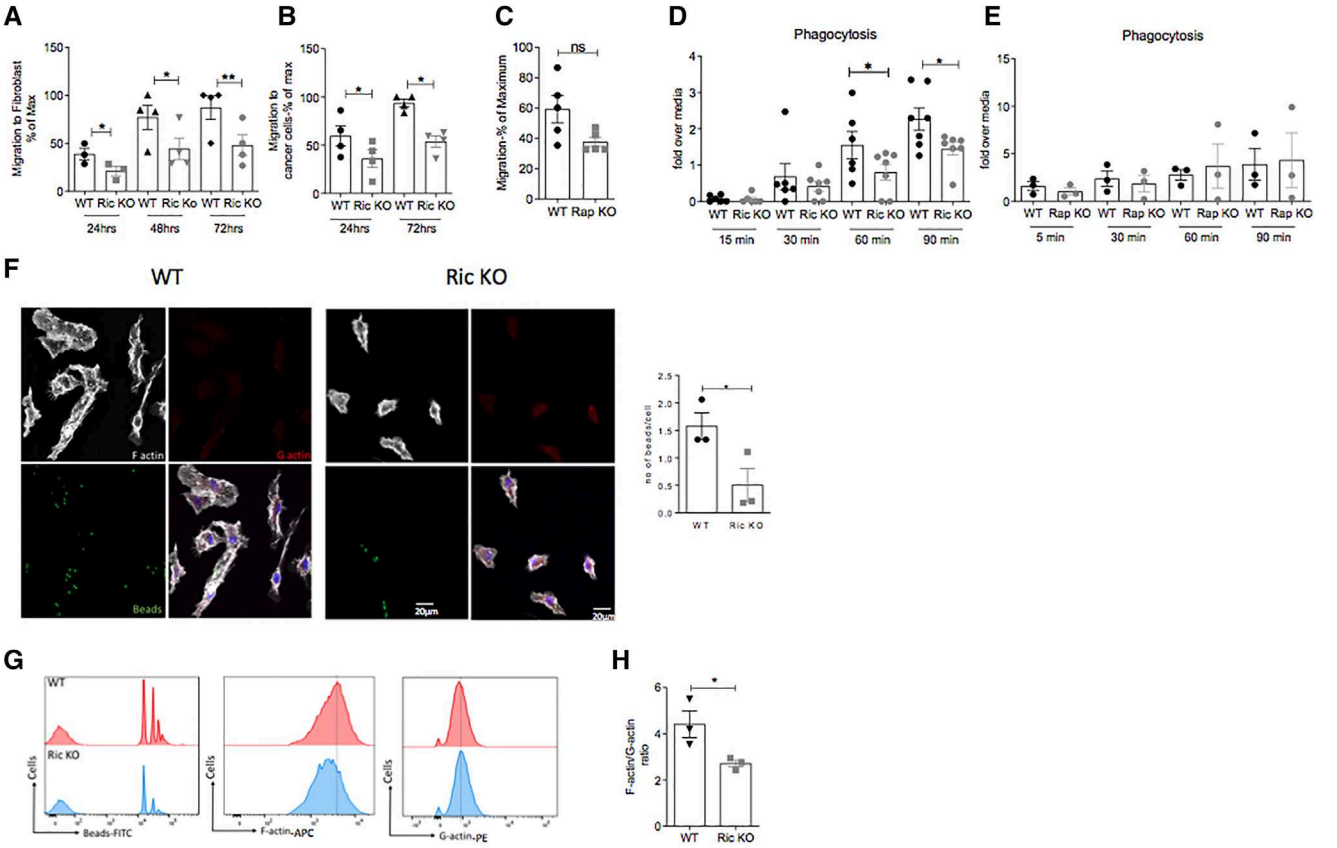

FIGURE 3 mTORC2 deficiency inhibits cytoskeletal rearrangement in macrophages. (A)–(C) BMDMs from WT or *CSF1R-icreER Rictor*^{ko} *or CSF1R-icreER Raptor*^{ko} mice were plated in 5 μm PET inserts against a chemoattractant gradient of mouse embryonic fibroblast cell line (MEFs) or (B) pancreatic tumor cells. BMDM migration was confirmed after 24, 48, and 72 h by fixing cells in 2% methanol and then dissolving in 10% acetic acid before measuring the absorbance e of the samples at 595 nm. Results shown as the % of max experiments were performed in triplicates and repeated with 3 or more biologic replicates. (D) and (E) WT and *CSF1R-icreER Rictor*^{ko} *or CSF1R-icreER Raptor*^{ko} BMDMs were treated with vehicle or LPS/IFNγ for 12 h. They were then incubated with IgG-coated carboxylate-modified flouromicrospheres for up to 90 min. The ingested particles were analyzed by flow cytometry and shown as MFI relative to media control. (F) Representative fluorescent image of F actin (white) and G actin (red) was also analyzed in macrophages after ingestion of microspheres (green). The number of ingested fluorescent particles were counted by confocal microscopy and presented as an average of 3 or more fields of vision. (G) Representative histogram of F actin (APC), g actin (PE), and fluorescent microspheres (FITC) during phagocytosis of microspheres. (H) MFI of F over g actin was analyzed as a ratio and displayed as bar graph. Experiments were repeated at least in 3 biologic replicates. Statistical test: unpaired *t*-test, $^{*}p < 0.05$

promigratory stimuli. Phagocytosis is another macrophage function where cytoskeletal rearrangements are required for the ingestion of external particles. As shown in Figure 3(D), phagocytosis of IgG-linked fluorescent particles was significantly reduced in CSF1R-icreER Rictor^{KO} BMDMs, while CSF1R-icreER Raptor^{KO} BMDMs ingested as efficiently as their WT counterparts (Figure 3(E)). We subsequently measured the ability of WT and Ric-deficient BMDMs to reorganize their actin cytoskeleton. Actin can be found in the cells as polymerized filamentous (F-actin) or globular nonpolymerized (G-actin) format. During cytoskeletal rearrangement, cells increase the F actin to G actin ratio. When analyzed and measured using immunofluorescence, a higher G actin staining and lower F/G actin ratio was detected in LPS-treated macrophages from CSF1R-cre Rictor^{KO} mice compared with CSF1R-cre Rictor^{WT} BMDMs (Figures 3(F)–3(H)). In addition, CSF1R-cre Rictor^{KO} BMDMs displayed a significantly different cell shape compared with WT BMDMs, possibly arising from inefficient filopodia and lamellipodia formation at the leading edge of the Rictor-deficient macrophages (Figure 3(F)).[27]

We conclude that the mTORC2 complex is a key regulator of cytoskeleton reorganization during monocyte/macrophage migration.

Rictor-deficient macrophages display altered signaling.

Most Rictor-mediated functions are dependent on mTORC2 ability to phosphorylate the kinase Akt at Serine 473.[28] We therefore assessed key signaling mediators downstream of Akt, which could underlie the functional phenotype of Rictor-deficient macrophages. BMDMs from CSF1R-icreER Rictor^{KO} and CSF1R-icreER Rictor^{WT} mice were stimulated in vitro with LPS/IFNγ at the indicated time points and lysates were analyzed by Western blot. As expected, phosphorylation of AKT at S473 was completely abolished in CSF1R-icreER Rictor^{KO} BMDMs (Figure 4(A)).

Furthermore, FoxO1 and FoxO4 phosphorylation, which are downstream of Akt signaling, were both significantly reduced in CSF1R-icreER Rictor^{KO} BMDMs (Figure 4(B)). Lack of FoxO1/4

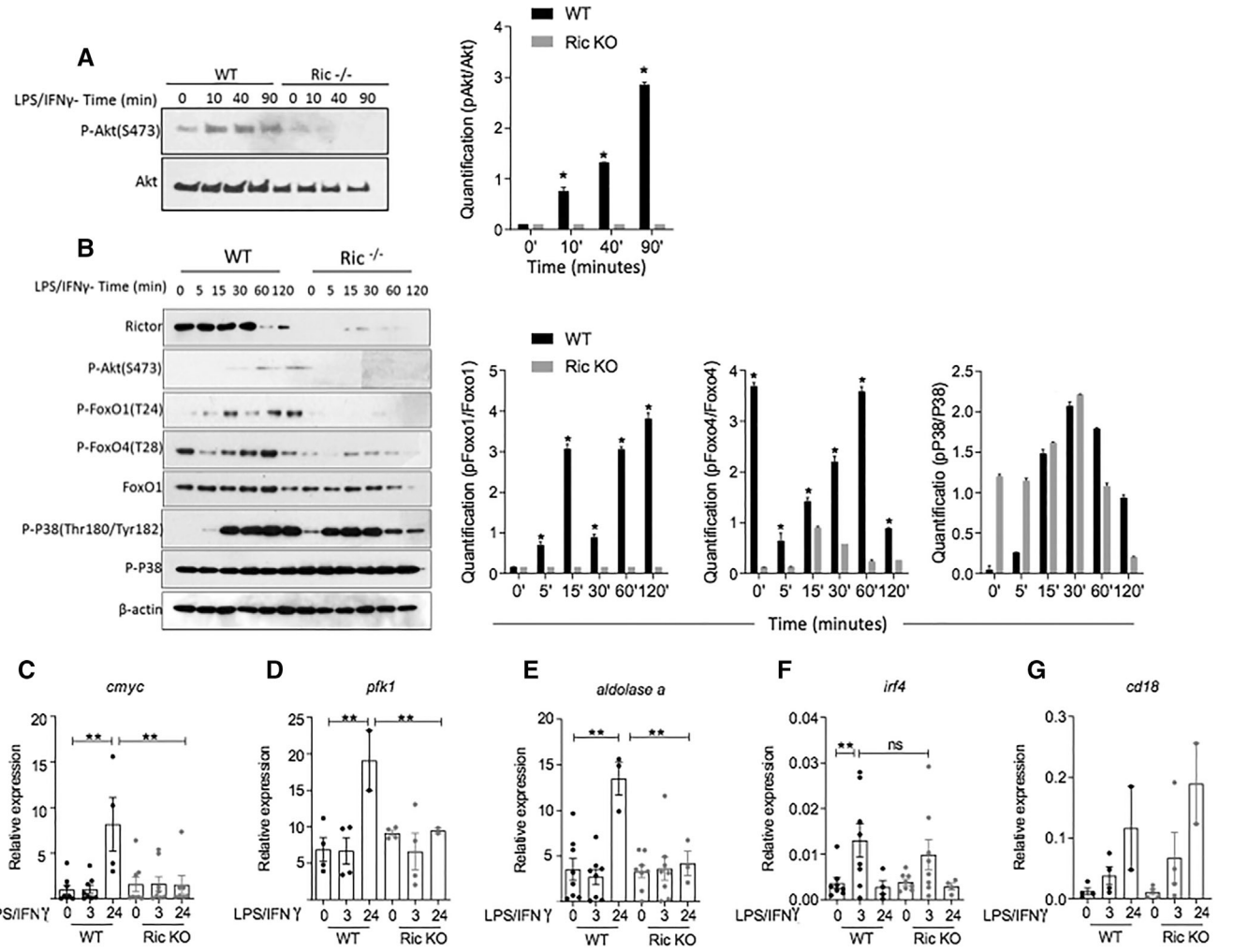

FIGURE 4 *CSF1R-icreER Rictor^{ko}* (Ric−/−) display defective Akt-dependent signaling pathways. (A) and (B) BMDMs stimulated with 100 ng/ml LPS and 20 ng/ml IFNγ. Expression of the indicated proteins was measured by Western blotting in a time-dependent (hours) manner in WT and *CSF1R-icreER Rictor^{ko}* (Ric−/−) protein lysates. The mean relative expression of proteins was measured by densitometric analysis in 3 independent experiments ± SD is shown. (') next to the numbers stands for the number of minutes. (C) The relative mRNA expression of *cmyc*, *pfk1*, *aldoalse a*, *irf4* and *cd18* by LPS/IFNγ-stimulated BMDMs after 0, 3, and 24 h was measured by RT-PCR. Data are shown as relative expression to the house keeping gene *rlp32* and show the mean ± SD of 3 independent experiments. Statistical test: unpaired *t*-test, $^{*}p < 0.05$; $^{***}p < 0.001$

phosphorylation results in their nuclear trapping and hence increased transcription of FoxO1/4 inflammatory target genes,[29] in line with the proinflammatory phenotype observed in LPS/IFNγ-stimulated CSF1R-icreER Rictor^{KO} macrophages (Figures 1(A)–1(E)).

Similar analyses were done on CSF1R-icreER Raptor^{KO} BMDMs. Phosphorylation of AKT at S473 remained intact in Raptor-deficient macrophages, while ribosomal protein S6 phosphorylation at S235-236 was significantly reduced (Figure S4). In these cells, greater IκB phosphorylation at S32 confirmed the previously described activation of the NFκB-mediated pathway and higher cytokine expression in CSF1R-icreER Raptor^{KO} BMDMs.[25] While efficient mTORC1 activity is indispensable for NF-κB activity in BMDMs, Rictor deficiency in CSF1R-icreER Rictor^{KO} BMDMs did not alter the phosphorylation levels of MAPK p38 (Figure 4(B))

The transcription factor c-Myc, a major regulator of cell metabolism and survival,[30] is required for the differentiation of alternatively activated (IL-4) macrophages[31] while its role in the differentiation of LPS/IFN-induced proinflammatory macrophages is unclear. Relevant to the observations above, c-Myc expression is modulated by mTORC2 through FoxO1-mediated phosphorylation and acetylation in glioblastoma cells which results in miRNA34c-dependent activation of c-Myc expression.[32]

RNA transcripts from LPS/IFNγ-treated CSF1R-icreER Rictor^{WT} and CSF1R-icreER Rictor^{KO} BMDMs were therefore analyzed by qPCR and a significant reduction of *cmyc* gene expression in CSF1R-icreER Rictor^{KO} macrophages was observed, compared with Rictor-expressing WT macrophages (Figure 4(C)). Aldolase-a and pfk are downstream target genes of c-Myc that are up-regulated during a glycolytic response.[33] In CSF1R-icreER Rictor^{WT} BMDMs, stimulation with LPS/IFNγ induced expression of both genes, which was significantly impaired in CSF1R-icreER Rictor^{KO} macrophages (Figures 4(D) and 4(E)).

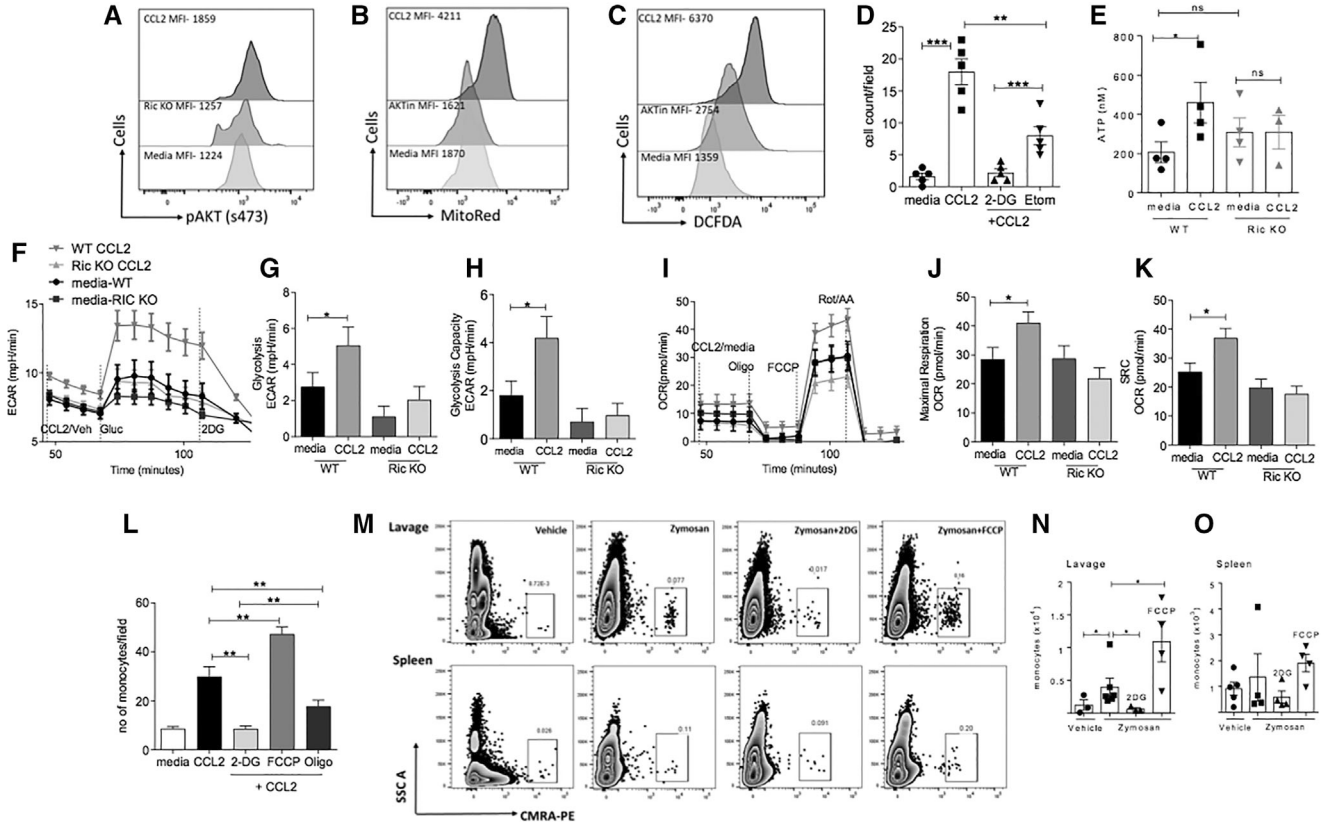

FIGURE 5 Metabolic regulation of migration in WT and CSF1R-icreER Rictor^{ko} (Ric KO) monocytes. (A) Primary bone marrow isolated monocytes from WT and *CSF1R-icreER Rictor^{ko}* (Ric KO) mice were treated with CCL2 or vehicle and pAKT-s473 expression was analyzed by intracellular FACS analysis and expressed as MFI. (B) and (C) MitoRed, (mitochondrial activation marker) and DCFDA (ROS production marker) expression in monocytes stimulated with CCL2 or vehicle ± AKT inhibitor were analyzed by flow cytometry. (D) WT monocytes were pretreated with either 2DG or etomoxir for 1 h and left to migrate through 5 μm-pore transwells in response to chemokine CCL2 for 2 h. Chemotaxis was measured by counting cells on the bottom of the transwell inserts. (E) ATP concentration of WT and *CSF1R-icreER Rictor^{ko}* monocyte lysates stimulated with vehicle or CCL2 for 2 h was analyzed in triplicates following manufacturer's instructions. (F)–(K) ECAR and OCR of monocytes stimulated live with either CCL2 or vehicle was measured by an extracellular flux analyzer (Seahorse). Medium was used as the control. Chemokines and glucose were added at the time points indicated (±SD experiments were done in $n = 6$ minimum with at least 3 biologic repeats). (I) Monocytes were isolated and prestimulated with vehicle, 2DG or FCCP and then allowed to transmigrate against a CCL2 gradient. (M)–(O) Isolated monocytes were prestimulated as shown and labeled with CMRA before being injected via tail vein to zymosan or vehicle treated mice. The absolute number of infiltrated monocytes into the peritoneal cavity was measured by flow cytometry analysis. Minimum 3 mice per group. Statistical test: unpaired *t*-test, $^{*}p < 0.05$, $^{*}p < 0.01$, $^{***}p < 0.001$

Expression of the transcription factor IRF4 has been recently shown to be dependent on mTORC2 signals during differentiation of alternatively activated macrophages,[34] where it promotes the glycolytic pathway. However, as shown in Figure 4(F), expression of IRF4 was not affected by Rictor deficiency in classically activated macrophages. Transcription of the integrin beta chain cd18 gene was also preserved in Rictor-deficient LPS/IFNγ-activated macrophages (Figure 4(G)). Since c-Myc is an upstream regulator, this ruled out any adhesion-dependent defects in Rictor-deficient macrophage motility.

Rictor is required for coupling of promigratory and promaturation stimuli with metabolic responses in monocytes.

We recently reported that the PI3K-mTORC2-Akt pathway sustains migration of regulatory T cells (Tregs) via induction of the hexokinase isoenzyme glucokinase.[3] Having observed that LPS/IFNγ-stimulated CSF1R-icreER Rictor^{KO} BMDMs have lower transcription of *aldolase-a* and *pfk* while also displaying impaired cytoskeletal recombination and migratory ability, we set out to investigate the contribution of the mTORC2-Akt pathway in reprogramming metabolism of migrating monocytes. Exposure of WT BMDMs to the chemokine CCL2 led to an increase in phosphorylation of Akt at S473 (Figure 5(A)), which, in contrast, remained at basal levels in CSF1R-icreER Rictor^{KO} monocytes. In addition, CCL2-induced Akt phosphorylation in WT monocytes was accompanied by enhanced mitochondrial activation and ROS production (Figures 5(B) and 5(C)).

Migration of monocytes pretreated either with vehicle, 2DG or etomoxir toward a CCL2 gradient was subsequently analyzed. 2DG is a glucose analogue that competitively inhibits glycolysis while etomoxir inhibits fatty acid oxidation and mitochondrial respiration (oxidative phosphorylation, oxphos). Both molecules significantly reduced the

migration of monocytes in response to CCL2 (Figure 5(D)), suggesting that monocytes require glycolysis and oxidative phosphorylation (oxphos) to sustain the energetic demands of migration.

We next compared ATP levels in these cells and observed that, after stimulation with CCL2, CSF1R-icreER Rictor^{WT} monocytes produced significantly more ATP than CSF1R-icreER Rictor^{KO} monocytes (Figure 5(E)). A real time analysis of the metabolic flux revealed a significantly reduced glycolytic response by *CSF1R-icreER Rictor^{KO}* monocytes compared with their WT counterpart in response to CCL2 (Figures 5(F)–5(H)). Specifically, CSF1R-icreER Rictor^{KO} monocytes displayed decreased glycolysis (Figure 5(G)) and glycolytic capacity (Figure 5(H)). Analysis of oxphos showed that the OCR was significantly higher after CCL2 addition in WT compared with Rictor-deficient monocytes (Figures 5(I)–5(K) and S5(A)). Maximal respiration (Figure 5(J)) and spare respiratory capacity (Figure 5(K)) were both reduced in CSF1R-cre Rictor^{KO} monocytes.

These results support a nonredundant role for mTORC2 in inducing the metabolic responses required for monocyte migration.

To investigate the relative contribution of aerobic glycolysis and oxphos to monocyte migration in vivo, monocytes from WT donors were isolated and then treated for 1 H with either vehicle, 2DG or FCCP, prior to adoptive transfer in mice which had previously received intraperitoneal zymosan injection. FCCP was used to disrupt the electron transport chain resulting in maximal cell respiration to compensate for ATP demand. This disruption also equilibrates the proton gradient in the cell rendering it more alkaline favoring cell migration through higher actin turnover.[35,36] Our results suggest that migration of adoptively transferred monocytes into the inflamed peritoneum was significantly reduced by 2DG pretreatment, confirming that monocytes rely upon glycolysis as the energy source to sustain their migratory activity. FCCP treatment enhanced their migration into the peritoneal cavity, highlighting the significance of oxidative phosphorylation and pH regulation on actin polymerization and cell migration (Figures 5(M)–5(O)).[36,37]

The observations made in vivo were confirmed by in vitro migration assays in which migration of 2DG pretreated monocytes was reduced, while FCCP enhanced CCL2-induced migration (Figure 5(L)).

Further, monocytes were pretreated with oligomycin and then analyzed for their migratory activity in response to CCL2. Oligomycin, an ATP synthase inhibitor, selectively inhibits oxidative phosphorylation and so is indicative of energy release through aerobic glycolysis. As shown in Figure 5(I), migration of oligomycin-treated monocytes to CCL2 was only partly reduced compared with migration of 2DG treated monocytes, suggesting that glycolysis can partly compensate for oxphos during monocyte migration, but not vice-versa.

We further sought to confirm the role of Akt activation in the events described above. Prior to exposure to CCL2, monocytes were treated with vehicle, 2DG and an Akt-selective inhibitor. Pharmacologic inhibition of Akt was also carried out in monocytes during treatment with FCCP and Oligomycin. As shown in Figure 6(A), inhibition of Akt phosphorylation reduced monocyte migration to levels similar to those elicited in the presence of 2DG. In addition, preventing Akt activation abrogated the enhancing effect of FCCP on monocyte migration and further increased the inhibitory effect of Oligomycin (Figure S5(B)).

In line with these results, qPCR analysis of monocytes exposed to CCL2 revealed a significant induction of several enzymes of the glycolytic pathway, TCA cycle and lipid metabolism, which were abrogated by inhibition of Akt signaling. Specifically, exposure to CCL2 significantly increased transcription of key enzymes of the glycolytic pathway, including *pkm2* and *enolase-2* as well as *c-Myc*, an upstream transcription factor, and *cpt1a*, a major fatty acid oxidation enzyme (Figures 6(B)–6(H)).

In line with our previous observation that the defective migration of Rictor-deficient monocytes is not due to a defect in expression of adhesion molecules, CD11a and CD18 expression was also unaffected by pharmacologic Akt inhibition (Figures 6(I) and 6(J)).

It has previously been shown that chemokines and integrins can induce monocyte maturation into macrophages.[38] We have shown that Rictor-deficient monocytes display reduced maturation following stimulation with LPS and IFNγ. To investigate the contribution of Akt-dependent metabolic switch in CCL2-treated monocyte maturation, monocytes were treated with CCL2 in the presence of the Akt inhibitor (triciribine), 2DG and etomoxir. MCSF was used as a positive control. As shown in Figure 7, CCL2 induced differentiation of BMDMs into F4/80-expressing macrophages. This event was prevented by both Akt and glycolysis inhibition. Etomoxir, an inhibitor of fatty acid oxidation and mitochondrial respiration did not significantly affect monocyte to macrophage differentiation.

As expected, zymosan per se did not induce monocyte maturation (Figure S6), suggesting that maturation of monocytes (Figure 2(C)) in response to this TLR2 ligand is indirectly mediated by cytokines and chemokines induced by TLR-2 signals.

Collectively, these data suggest that Akt activation by mTORC2 is required to maintain the energy supply required for monocyte migration and maturation.

4 | DISCUSSION

The results described here show that loss of mTORC2 activity in myeloid cells enhances the proinflammatory phenotype of classically activated macrophages with increased release of proinflammatory cytokine including NOS2, IL-6, and IL-12 in Rictor-deficient macrophages stimulated with TLR ligands. Mechanistically, our investigation points to the induction of Akt-mediated nuclear exclusion of FoxO1 to account for this effect, in line with previous findings showing that Akt activation prevented FoxO1-mediated inhibition of TLR4 target gene transcription.[39,40] More recently, Katholnig et al.[41] also showed that loss of mTORC2 is accompanied with a more proinflammatory macrophage signature that induces colitis and tumor growth in mice.

Despite the proinflammatory phenotype in vitro, monocyte/macrophage specific Rictor deficiency results in an anti-inflammatory phenotype in vivo. Our data indicate that this phenotype is at least in part due to defective migration and maturation

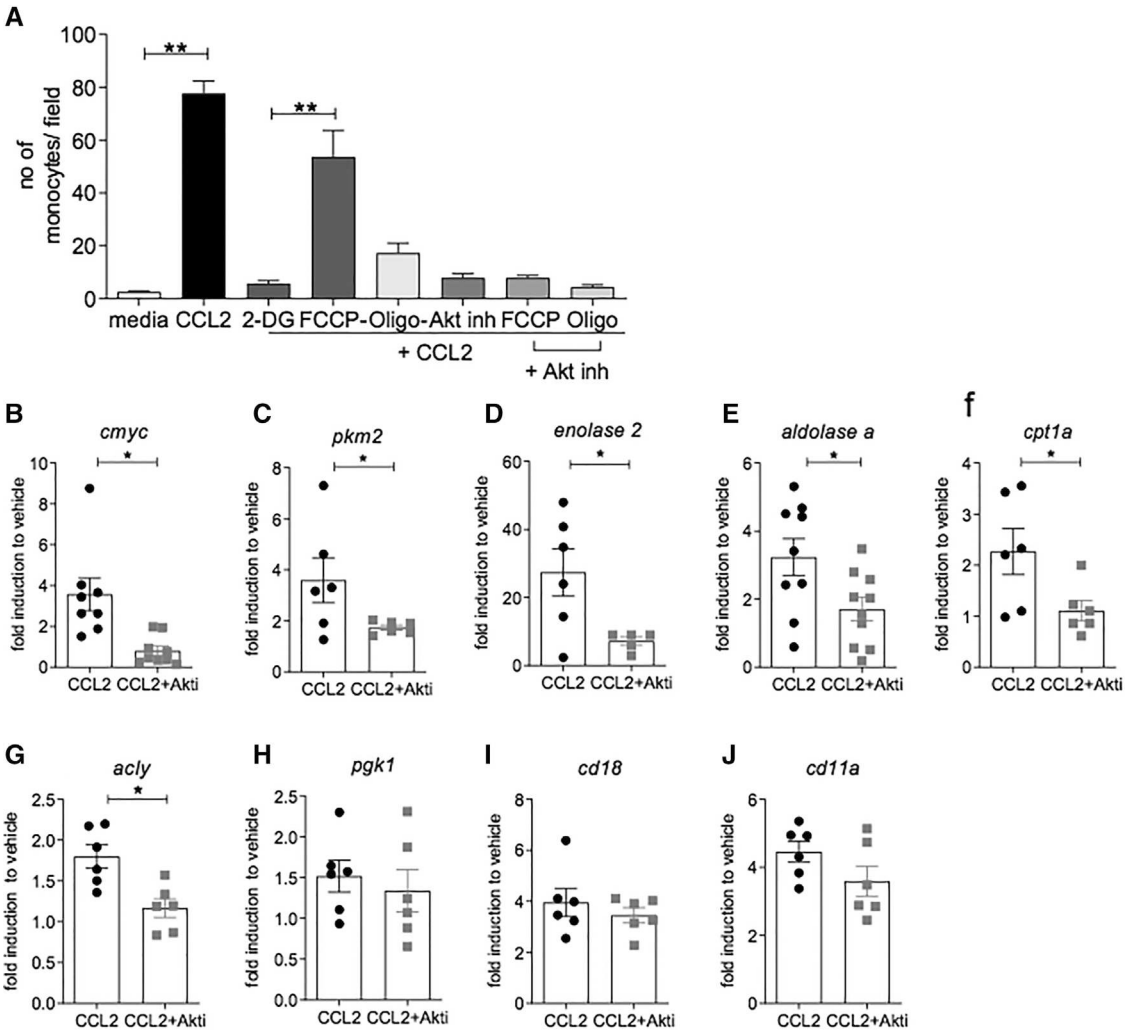

FIGURE 6 Akt-dependent regulation of metabolic gene expression in CCL2-stimulated monocytes. (A) WT monocytes were pretreated with either 2DG, FCCP or oligomycin ± AKT inhibitor for 1 h and left to migrate through 5 μm-pore transwells in response to chemokine CCL2 for 2 h. Chemotaxis was measured by counting cells on the bottom of the transwell inserts. (B)–(I) The relative mRNA expression of *cmyc* (B), *pkm2* (C), *enolase 2* (D), *aldoalse a* (E), *cpt1a* (F), *acly* (G), *pgk1* (H), *cd18* (I), and *cd11a* (J) by CCL2-stimulated monocytes was measured by RT-PCR. Data are shown as relative expression to the house keeping gene *rlp32* and show the mean value of 3 independent experiments ± SD. Statistical test: unpaired *t*-test, $^{**}p < 0.001$

of monocytes in tissue, resulting from an overall impairment of cytoskeleton dynamics sustaining migration, maturation, and phagocytosis. Clearance of inflammatory dying cancer cells is required for efficient antitumor response.[42] It is suspected therefore that our Rictor-deficient macrophages illustrating defective phagocytosis could be important mediators in observing significantly larger tumors in CSF1R-icreER Rictor^{KO} mice.

Importantly, impaired actin reorganization dynamics in Rictor-deficient monocyte/macrophages results from a defective metabolic adaptation and energy supply in response to promigratory stimuli, such as chemokines. Specifically, we found that Rictor deficiency results in a significant decrease in glycolysis and oxidative phosphorylation, leading to reduced ATP and ROS production in CCL2-stimulated monocytes. Our experiments also indicate that this metabolic reprogramming is Akt dependent. One possible explanation is that, through Akt-dependent induction of FoxO phosphorylation and acetylation,[32] mTORC2 activation induces the expression of c-Myc, a master regulator of glycolysis, and subsequently the transcription of c-Myc-target genes such *pkm2*[43] and *alpha-enolase*.[44]

Through c-Myc activity, and specifically by enhancing transcription of genes encoding for carnitine palmitoyltransferase (CPT1a) and ATP citrate lyase (ACLY), the mTORC2-Akt pathway might also promote oxidative phosphorylation in migrating monocytes. CPT1a is required for the transport of fatty acids into the mitochondria, where they undergo oxidation. Pyruvate, produced by the glycolytic pathway, can feed into aerobic glycolysis as well as TCA cycle through ACLY activity.[45] ACLY activity has been linked to increased glucose consumption and higher NO and ROS production in macrophages[45,46] and has been linked to efficient macrophage differentiation and polarization through increased acetylation of genes in alternatively

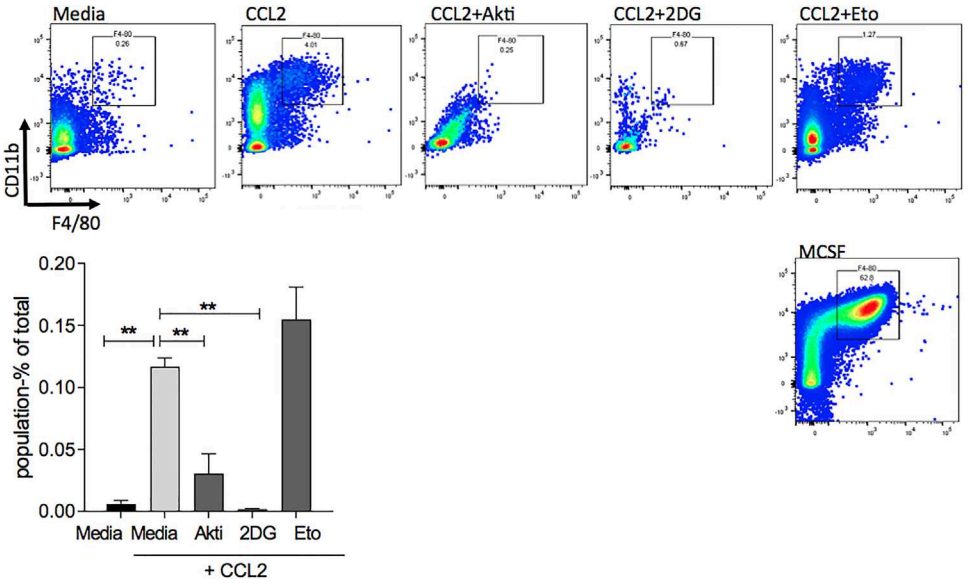

FIGURE 7 Chemokine-mediated monocyte to macrophage differentiation is regulated by AKT-dependent metabolic reprograming. Bone marrow derived cells were stimulated with media only or CCL2 in the presence of the indicated inhibitors. The percentage of CD11b^{hi} F480+ macrophages were analyzed by flow cytometry and shown as the mean percentage of total cells ± SD. Statistical test: unpaired *t*-test, $^{**}p < 0.01$

activated macrophages.[47] Further studies will be needed to challenge this hypothesis.

Reduced oxphos as a consequence of Rictor deficiency did not affect monocyte migration as much as the impairment of the glycolytic flux. While the full functional consequences of mTORC2 regulation of macrophage oxphos remain to be fully investigated, the partial effect on migration can be explained by the failure of upstream glycolysis to engage oxphos, while ATP can still be produced by aerobic glycolysis independently of mitochondrial respiration.

Despite being functionally proinflammatory, Rictor-deficient, classically activated macrophages also displayed maturation defects illustrated by lower CD64, CD86, and F4/80 molecule expression. In addition, CCL2-induced maturation of monocytes in nonpolarizing conditions was substantially reduced following Akt and glycolysis inhibition, suggesting that mTORC2-induced, Akt-mediated regulation of metabolic responses is required in the early events of macrophage-mediated immunity, namely monocyte migration and maturation. In a recent study, Rictor deficiency in TLR4-activated dendritic cells (DCs) led to enhanced IL-6 and IL-23 expression but also lower B7-H1 and CD40 expression.[48]

Rictor deficiency in alternatively activated macrophages leads to a proinflammatory phenotype in vivo, suggesting that monocytes undergoing M2-like differentiation do not depend on Rictor to migrate into tissues. It is possible that these cells rely upon other signaling pathways to meet the energy demands of migration, while silencing of Rictor signaling is necessary for the development of M1-like function, independently of the environmental cues. Subsequently, continued mTORC2 activity in alternatively activated macrophages may promote the acquisition of an anti-inflammatory phenotype. In alternatively activated macrophages, mTORC2 has been shown to operate in parallel with the IL-4Ra-Stat6 pathway to facilitate increased glycolysis during M2 activation via the induction of the transcription factor IRF4.[34] Our investigation shows that IRF4 transcription was not reduced in Rictor-deficient, classically activated macrophages suggesting that Rictor induces different transcriptional programs to increase glycolysis in M1 and M2-like macrophages, macrophages, which could explain the lack of effect of Rictor deficiency on migration and maturation of alternatively activated monocytes.

Besides revealing a distinct transcriptional programme downstream of Rictor in classically and alternatively differentiated macrophages, our study is relevant to the recent interest in the development of mTORC2 selective inhibitors in cancer therapy.[49] Based in part on the proinflammatory effects on monocyte differentiation,[50,17] it has been proposed that selective inhibitors of mTORC1 and 2 may be effective anti-cancer drugs.[51] Our data suggest that this might be a flawed approach, as the increased inflammatory phenotype elicited by loss of mTORC2 activity may be outweighed by the inability of monocytes to reach the tumor tissue and differentiate.

ACKNOWLEDGMENTS

This study was funded by the British Heart Foundation (CH/15/2/32064 and RG/14/2/30616 to F.M.-B.) and Cancer Research UK (14355, 16354, and 25714 to F.B.). The Seahorse Analyzer X was funded by the British Heart Foundation (CH/15/2/32064 to F.M.-B.).

DISCLOSURES

The authors declare no conflict of interests.

AUTHORSHIP

M.J. performed most of the experiments; L.Y. and E.J.W. performed the experiments; M.J., L.Y., E.J.W., and S.N. analyzed the data; M.J.,

M.C., F.B., and F.M.-B. designed the experiments; M.J., M.C., F.B., and F.M.-B. wrote the manuscript. All authors discussed and revised the manuscript.

REFERENCES

1. Shi C, Pamer EG. Monocyte recruitment during infection and inflammation. *Nat Rev Immunol*. 2011;11:762-774.
2. Chiu S, Bharat A, Role of monocytes and macrophages in regulating immune response following lung transplantation. *Curr Opin Org Transplant* 21, 239-245, https://doi.org/10.1097/MOT.0000000000000313 (2016).
3. Kishore M, Cheung KCP, Fu H, et al, Regulatory T cell migration is dependent on glucokinase-mediated glycolysis. *Immunity* 47, 875-889.e810, https://doi.org/10.1016/j.immuni.2017.10.017 (2017).
4. Geissmann F, Manz MG, Jung S, Sieweke MH, Merad M, Ley K. Development of monocytes, macrophages, and dendritic cells. *Science*. 2010;327:656.
5. Ingersoll MA, Platt AM, Potteaux S, Randolph GJ. Monocyte trafficking in acute and chronic inflammation. *Trends Immunol*. 2011;32:470-477.
6. Covarrubias AJ, Aksoylar HI, Horng T. Control of macrophage metabolism and activation by mTOR and Akt signaling. *Semin Immunol*. 2015;27:286-296.
7. Troutman TyD, Bazan JF, Pasare C. Toll-like receptors, signaling adapters and regulation of the pro-inflammatory response by PI3K. *Cell Cycle*. 2012;11:3559-3567.
8. Ruse M, Knaus UG. New players in TLR-mediated innate immunity: pI3K and small Rho GTPases. *Immunol Res*. 2006;34:33-48.
9. Luyendyk JP, Schabbauer GA, Tencati M, Holscher T, Pawlinski R, Mackman N. Genetic analysis of the role of the PI3K-Akt pathway in lipopolysaccharide-induced cytokine and tissue factor gene expression in monocytes/macrophages. *J Immunol (Baltimore, Md : 1950)*. 2008;180:4218-4226.
10. Mills EL, O'neill LA. Reprogramming mitochondrial metabolism in macrophages as an anti-inflammatory signal. *Eur J Immunol*. 2016;46:13-21.
11. Linke M, Fritsch SD, Sukhbaatar N, Hengstschläger M, Weichhart T. mTORC1 and mTORC2 as regulators of cell metabolism in immunity. *FEBS Lett*. 2017;591:3089-3103.
12. Byles V, Covarrubias AJ, Ben-Sahra I, et al. The TSC-mTOR pathway regulates macrophage polarization. *Nat Commun*. 2013;4:2834.
13. Pan H, O'brien TF, Zhang P, Zhong X-P. The role of tuberous sclerosis complex 1 in regulating innate immunity. *J Immunol*. 2012;188:3658.
14. Weichhart T, Hengstschläger M, Linke M. Regulation of innate immune cell function by mTOR. *Nat Rev Immunol*. 2015;15:599.
15. Cheng S-C, Quintin J, Cramer RA, et al. mTOR- and HIF-1alpha-mediated aerobic glycolysis as metabolic basis for trained immunity. *Science*. 2014;345:1250684.
16. Moon J-S, Hisata S, Park Mi-Ae, et al. mTORC1-induced HK1-dependent glycolysis regulates NLRP3 inflammasome activation. *Cell Rep*. 2015;12:102-115.
17. Huang SC-C, Smith AM, Everts B, et al. Metabolic reprogramming mediated by the mTORC2-IRF4 signaling axis is essential for macrophage alternative activation. *Immunity*. 2016;45:817-830.
18. Oh M-H, Collins SL, Sun Im-H, et al. mTORC2 signaling selectively regulates the generation and function of tissue-resident peritoneal macrophages. *Cell Rep*. 2017;20:2439-2454.
19. Festuccia WT, Pouliot P, Bakan I, Sabatini DM, Laplante M. Myeloid-specific Rictor deletion induces M1 macrophage polarization and potentiates in vivo pro-inflammatory response to lipopolysaccharide. *PLoS One*. 2014;9:e95432-e95432.
20. Fogg DK. A clonogenic bone marrow progenitor specific for macrophages and dendritic cells. *Science*. 2006;311:83-87.
21. Perdiguero EG, Geissmann F. The development and maintenance of resident macrophages. *Nat Immunol*. 2016;17:2-8.
22. Livak KJ, Schmittgen TD. Analysis of relative gene expression data using real-time quantitative PCR and the 2(-Delta Delta C(T)) method. *Methods*. 2001;25(4):402–408. https://doi.org/10.1006/meth.2001.1262.
23. Qian B-Z, Li J, Zhang H, et al. CCL2 recruits inflammatory monocytes to facilitate breast-tumour metastasis. *Nature*. 2011;475:222-225.
24. Vergadi E, Ieronymaki E, Lyroni K, Vaporidi K, Tsatsanis C. Akt signaling pathway in macrophage activation and M1/M2 polarization. *J Immunol*. 2017;198:1006.
25. Weichhart T, Costantino G, Poglitsch M, et al. The TSC-mTOR signaling pathway regulates the innate inflammatory response. *Immunity*. 2008;29:565-577.
26. Sato M, Sano H, Iwaki D, et al. Direct binding of Toll-like receptor 2 to zymosan, and zymosan-induced NF-κB activation and TNF-α secretion are down-regulated by lung collectin surfactant protein A. *J Immunol*. 2003;171:417.
27. Ridley AJ. Life at the leading edge. *Cell*. 2011;145:1012-1022.
28. Ikenoue T, Inoki K, Yang Q, Zhou X, Guan K-L. Essential function of TORC2 in PKC and Akt turn motif phosphorylation, maturation and signalling. *EMBO J*. 2008;27:1919-1931.
29. Fan W, Morinaga H, Kim JJ, et al. FoxO1 regulates Tlr4 inflammatory pathway signalling in macrophages. *EMBO J*. 2010;29:4223-4236.
30. Dang CV, Le A, Gao P. MYC-induced cancer cell energy metabolism and therapeutic opportunities. *Clin Cancer Res*. 2009;15:6479.
31. Mantovani A, Locati M. Orchestration of macrophage polarization. *Blood*. 2009;114:3135-3136.
32. Masui K, Tanaka K, Akhavan D, et al. mTOR complex 2 controls glycolytic metabolism in glioblastoma through FoxO acetylation and upregulation of c-Myc. *Cell Metab*. 2013;18:726-739.
33. Chang Y-C, Yang Y-C, Tien C-P, Yang C-J, Hsiao M. Roles of aldolase family genes in human cancers and diseases. *Trends Endocrinol Metab*. 2018;29:549-559.
34. Huang SC-C, Smith AM, Everts B, et al. Metabolic reprogramming mediated by the mTORC2-IRF4 signaling axis is essential for macrophage alternative activation. *Immunity*. 2016;45:817-830.
35. Schwab A, Stock C. Ion channels and transporters in tumour cell migration and invasion. *Philos Trans R Soc Lond B Biol Sci*. 2014;369:20130102-20130102.
36. Yonezawa N, Nishida E, Sakai H. pH control of actin polymerization by cofilin. *J Biol Chem*. 1985;260:14410-14412.
37. Frantz C, Barreiro G, Dominguez L, et al. Cofilin is a pH sensor for actin free barbed end formation: role of phosphoinositide binding. *J Cell Biol*. 2008;183:865-879.
38. Schraufstatter IU, Zhao M, Khaldoyanidi SK, Discipio RG. The chemokine CCL18 causes maturation of cultured monocytes to macrophages in the M2 spectrum. *Immunology*. 2012;135:287-298.
39. Fan W, Morinaga H, Kim JJ, et al. FoxO1 regulates Tlr4 inflammatory pathway signalling in macrophages. *EMBO J*. 2010;29:4223-4236.
40. Brown J, Wang H, Suttles J, Graves DT, Martin M. Mammalian target of rapamycin complex 2 (mTORC2) negatively regulates Toll-like receptor 4-mediated inflammatory response via FoxO1. *J Biol Chem*. 2011;286:44295-44305.
41. Katholnig K, Schütz B, Fritsch SD, et al. Inactivation of mTORC2 in macrophages is a signature of colorectal cancer that promotes tumorigenesis. *JCI Insight*. 2019;4:e124164.
42. Werfel TA, Cook RS. Efferocytosis in the tumor microenvironment. *Semin Immunopathol*. 2018;40:545-554.
43. Masui K, Cavenee WK, Mischel PS. S. mTORC2 in the center of cancer metabolic reprogramming. *Trends Endocrinol Metab*. 2014;25:364-373.
44. Feo S, Arcuri D, Piddini E, Passantino R, Giallongo A. ENO1 gene product binds to the c-myc promoter and acts as a transcriptional repressor: relationship with Myc promoter-binding protein 1 (MBP-1). *FEBS Lett*. 2000;473:47-52.

45. Kelly B, O'neill LAj. Metabolic reprogramming in macrophages and dendritic cells in innate immunity. *Cell Res*. 2015;25:771.
46. Infantino V, Iacobazzi V, Palmieri F, Menga A. ATP-citrate lyase is essential for macrophage inflammatory response. *Biochem Biophys Res Commun*. 2013;440:105-111.
47. Covarrubias AJ, Aksoylar HI, Yu J, et al. Akt-mTORC1 signaling regulates Acly to integrate metabolic input to control of macrophage activation. *Elife*. 2016;5.
48. Raïch-Regué D, Rosborough BR, Watson AR, Mcgeachy MJ, Turnquist HR, Thomson AW. mTORC2 deficiency in myeloid dendritic cells enhances their allogeneic Th1 and Th17 stimulatory ability after TLR4 ligation in vitro and in vivo. *J Immunol*. 2015;194:4767.
49. Zou Z, Chen J, Yang J, Bai X. Targeted inhibition of Rictor/mTORC2 in cancer treatment: a new era after rapamycin. *Curr Cancer Drug Targets*. 2016;16:288-304.
50. Zhao Y, Shen X, Na N, et al. mTOR masters monocyte development in bone marrow by decreasing the inhibition of STAT5 on IRF8. *Blood*. 2018;131:1587-1599.
51. Sparks CA, Guertin DA. Targeting mTOR: prospects for mTOR complex 2 inhibitors in cancer therapy. *Oncogene*. 2010;29:3733-3744.

SUPPORTING INFORMATION

Additional supporting information may be found in the online version of the article at the publisher's website.

How to cite this article: Jangani M, Vuononvirta J, Yamani L, et al. Loss of mTORC2-induced metabolic reprogramming in monocytes uncouples migration and maturation from production of proinflammatory mediators. *J Leukoc Biol*. 2022;111:967–980.
https://doi.org/10.1002/JLB.1A0920-588R